engineering proceedings

MDPI

Proceeding Paper

Optimized Shoot-Through Pulse Generation in High Voltage Boost Z-Source Inverters: A Performance-Based PWM Technique Comparison †

Sweta Kumari [1,*], Rajib Kumar Mandal [2] and S. P. Daniel Chowdhury [3,4]

[1] Electrical Engineering Department, Government Engineering College, Siwan 841226, Bihar, India
[2] Electrical Engineering Department, National Institute of Technology, Patna 800004, Bihar, India; rajib@nitp.ac.in
[3] School of Engineering, Independent Institute of Education (IIEMSA), Johannesburg 1724, South Africa; spchowdhury2010@gmail.com
[4] S5 Enterprises (Pty) Ltd., Cape Town 7700, South Africa
* Correspondence: swetak.phd18.ee@nitp.ac.in
† Presented at the 34th Southern African Universities Power Engineering Conference (SAUPEC 2026), Durban, South Africa, 30 June–1 July 2026.

Abstract

Z-source inverters (ZSIs) provide single-stage power conversion with inherent voltage boost capability through shoot-through (ST) states achieved using specialized PWM methods. This study compares various ST PWM strategies, Simple Boost PWM, Maximum Boost PWM, Constant Boost Third Harmonic Injection PWM, and Space Vector PWM, for high-voltage boost ZSI (HVB-ZSI) applications. A MATLAB/Simulink 2024a model was developed to assess their performance in terms of output-voltage quality, THD, capacitor-voltage stress, switch stress, and inductor–current ripple. Results indicate that while all techniques enable ST operation effectively, their voltage stress and harmonic performance differ notably, guiding optimal PWM selection for advanced ZSI-based systems.

Keywords: high voltage boost ZSI; PWM; THD; shoot-through control

1. Introduction

Renewable energy sources such as solar panels and wind turbines generate electricity at variable voltage levels due to changing environmental conditions like sunlight and wind speed [1,2]. To efficiently deliver this electricity to the grid or connected loads, it is often necessary to increase the voltage [3]. Boosting the voltage helps match the output of renewable sources with the required grid or load voltage. This not only ensures proper power transfer but also reduces transmission losses and improves the overall efficiency of the system. Electricity grids operate at fixed, standardized voltage levels. Therefore, to integrate renewable energy systems smoothly into the grid, it is important to adjust the output voltage of these sources to match the grid voltage. High voltage boost converters are used to achieve this, making the connection between renewable sources and the grid more reliable and efficient [4].

The Z-source inverter (ZSI) has emerged as a significant innovation in power conversion technology, offering an integrated solution for both voltage boost and inversion in a single stage [5,6]. This makes ZSI highly suitable for renewable energy applications where voltage boosting is required. Due to this unique capability, ZSI has gained significant attention in recent years for high-voltage applications. An upgraded version of this

Check for updates

Academic Editor: Akshay Kumar Saha

Published: 12 May 2026

Copyright: © 2026 by the authors. Licensee MDPI, Basel, Switzerland. This article is an open access article distributed under the terms and conditions of the Creative Commons Attribution (CC BY) license.

converter, known as the improved High Voltage Boost Z-Source Inverter (HVB-ZSI), has been proposed in [7] to further enhance voltage gain and system performance. It employs an input capacitor and active switches to make the current in the Z-source network flow in the reverse direction, which makes the inverter not only have high boost capacity but also can adapt to a wide range of load changes. The structure and operational principles of the improved ZSI model are presented in the subsequent sections of this article.

Whereas Pulse Width Modulation (PWM) plays a pivotal role in the control of power electronic converters, particularly in ZSIs, where it governs both the shoot-through (ST) state and overall power conversion efficiency [8]. In ZSIs, ST states are deliberately introduced within the switching cycle to enable voltage boosting [9]. The way these ST pulses are generated and inserted into the switching sequence directly impacts the inverter's voltage gain, switching stress, better harmonic performance, and improved system stability [10]. Over time, several PWM techniques have been developed to effectively manage ST states in ZSIs. Among the commonly used methods are Simple Boost PWM (SBPWM), Maximum Boost Control PWM (MBCPWM), Third Harmonic Injection-based Constant Boost Control PWM (THI-CBCPWM), and Space Vector PWM (SVPWM). Each technique has its own operating principle and suitability depending on the application needs.

Although several PWM techniques have been developed for ST control in conventional ZSIs, there is a lack of focused studies that compare their performance when applied to advanced high-voltage gain ZSI topologies. This creates a research gap in understanding which modulation technique provides optimal performance for such enhanced ZSI architectures. This study centers around a newly proposed ZSI topology with enhanced boost capability, offering key advantages, such as reduced voltage stress on the Z-source capacitors and effective limitation of inrush current during startup. Various PWM-based modulation techniques are considered for generating ST pulses suitable for this high-gain configuration. A comprehensive discussion is carried out on the control methodology and its impact on overall inverter performance. Comparative analysis of different ST control strategies is presented, and the proposed approach is evaluated using detailed simulation studies in the MATLAB/Simulink 2024a environment to demonstrate its performance and suitability for advanced power-conversion applications. The novelty of this work is the development and implementation of an optimized ST pulse generation strategy for an HVB-ZSI.

2. HVB-ZSI

The newly developed improved high-gain ZSI topology presents an efficient and intelligent solution for achieving substantial voltage boosting without introducing additional system complexity [7]. One of the key advantages of this design is its ability to generate significantly higher output voltage even with minimal ST duration, thereby enhancing efficiency while reducing switching stress. A major improvement lies in the considerable reduction in voltage stress on both the inverter bridge and the Z-source capacitors. This not only minimizes the likelihood of component failure but also extends the operational lifespan of critical components, leading to improved system reliability. Furthermore, this inverter topology incorporates inherent protection against high inrush currents during startup. An additional innovation is the integration of an input capacitor and an active switch within the impedance network. This configuration enables current reversal within the Z-source network, thereby enhancing the inverter's adaptability to varying load conditions. The ability to handle reverse current effectively allows the system to respond rapidly to dynamic power demands, making it highly suitable for applications such as renewable energy systems and electric drives. The circuit configuration of the HVB-ZSI is illustrated in Figure 1.

https://doi.org/10.3390/engproc2026140007

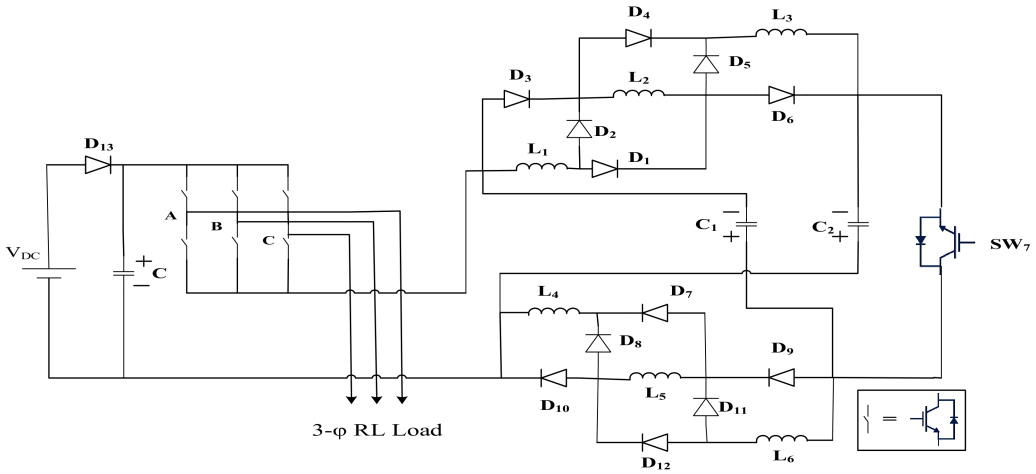


Figure 1. Circuit configuration of HVB-ZSI.

The various modes of operation of the enhanced HVB-ZSI are systematically analyzed to understand its dynamic behavior under diverse operating conditions. This analysis focuses on how the inverter responds to variations in load and switching sequences, thereby highlighting its superior performance and adaptability compared to conventional ZSI topologies. The enhanced HVB-ZSI operates through three distinct switching states:

- ST Zero-Vector State: Both switches in a phase leg are turned on, enabling energy transfer from inductors to capacitors for voltage boosting.
- Conventional Zero-Vector States: All upper or all lower switches are on, resulting in zero output voltage while supporting power balance and ST timing.
- Active Vector States: These states transfer power to the AC load, shaping the output waveform and enabling high voltage gain with enhanced modulation control.

The eight switching states of HVB-ZSI, as illustrated through corresponding circuit models in [7], encompass ST zero-vector states, conventional zero-vector states, and active vector states.

In Figure 1, the following assumptions are made for simplification: the capacitors are equal, i.e., $C_1 = C_2$; all inductors are identical, i.e., $L_1 = L_2 = L_3 = L_4 = L_5 = L_6$; and the corresponding capacitor and inductor voltages are also equal, i.e., $V_{C1} = V_{C2} = V_C$ and $V_{L1} = V_{L2} = V_{L3} = V_{L4} = V_{L5} = V_{L6} = V_L$. With these assumptions in place, the ZSI's operating states can be described as follows:

State 1: In this ST state, the inductors store energy while the capacitors discharge, resulting in the inductor voltage expressed as,

$$V_L = V_{DC} + V_C \tag{1}$$

State 2: The inverter continues to operate in the ST zero-vector mode. During this state, the capacitors in the Z-source network, along with the input capacitor, work together to charge the inductors. As a result, the current through the inductors begins to rise in the positive direction.

State 3: The inverter transitions to a conventional zero-vector state, and the inverter delivers no active power to the load as switches maintain a non-conducting or balanced state. During this state, the input voltage is given by Equation (2) and the total inductor voltage satisfies Equation (3), indicating energy transfer from capacitors to inductors.

$$V_{in} = V_{DC} + 2V_C \tag{2}$$

$$3V_L = -V_C \tag{3}$$

State 4: In active vector state, the inverter delivers power to the load by generating a non-zero output voltage through proper switching. In this state; the diode current, $i_D > 0$ and $i_L > i_{in}$, also the input voltage is expressed as per Equation (4), indicating continued voltage boost and energy transfer.

$$V_{in} = V_{DC} + 2V_C \tag{4}$$

State 5: During this state, the inverter effectively transfers power to the load, with inductor current bounded as, $\frac{1}{2} i_{in} < i_L < i_{in}$ ensuring controlled energy delivery and stable operation.

State 6: In this operating condition, the inductor current lies within the range $0 < i_L < \frac{1}{2} i_{in}$, indicating partial energy storage in the inductors and minimal contribution to load power.

State 7: The inverter remains in the active vector state, with switch SW_7 continuing to stay closed, allowing sustained power transfer and maintaining the desired current flow within the circuit.

State 8: The inverter is operating in the standard zero-vector mode, where the output voltage is zero and the switching devices are arranged to maintain a neutral state without delivering power to the load.

The final expressions establish the key voltage relationships in the HVB-ZSI [7]. The capacitor voltage is defined by Equation (5), the DC-link voltage by Equation (6), and the boost factor by Equation (7), clearly illustrating how the ST duty ratio d_{st} influences voltage boosting. These equations are derived by systematically simplifying the circuit models corresponding to switching states 1 through 8.

$$V_C = \frac{3\, d_{st}}{1 - 4 d_{st}}\, V_{DC} \tag{5}$$

$$V_{in} = \frac{1 + 2\, d_{st}}{1 - 4\, d_{st}}\, V_{dc} = B V_{DC} \tag{6}$$

$$B = \frac{1 + 2\, d_{st}}{1 - 4\, d_{st}} \tag{7}$$

3. Overview of PWM Approaches

In the context of ZSIs, PWM techniques are not only responsible for voltage regulation but also for embedding ST states. The way these ST intervals are generated and positioned within the switching cycle directly affects the inverter's boost factor, capacitor stress, efficiency, and harmonic performance [11]. In this study, different PWM strategies are evaluated for an HVB-ZSI topology. The goal is to determine which modulation approach is most compatible and efficient for this improved inverter architecture.

3.1. Simple Boost Control PWM (SBPWM)

In SBPWM, with $0 < d_{st} < 0.5$, the ST pulses are inserted in the zero-vector time of the traditional PWM waveform, which reduces the available time for active switching vectors, thereby limiting the modulation index (M). One of the main advantages of SBPWM is its simplicity in implementation, as it does not require complex reference-signal generation or space-vector calculations [12]. Figure 2 shows the switching diagram of the SBPWM switching sequence applied to the HVB-ZSI.

https://doi.org/10.3390/engproc2026140007

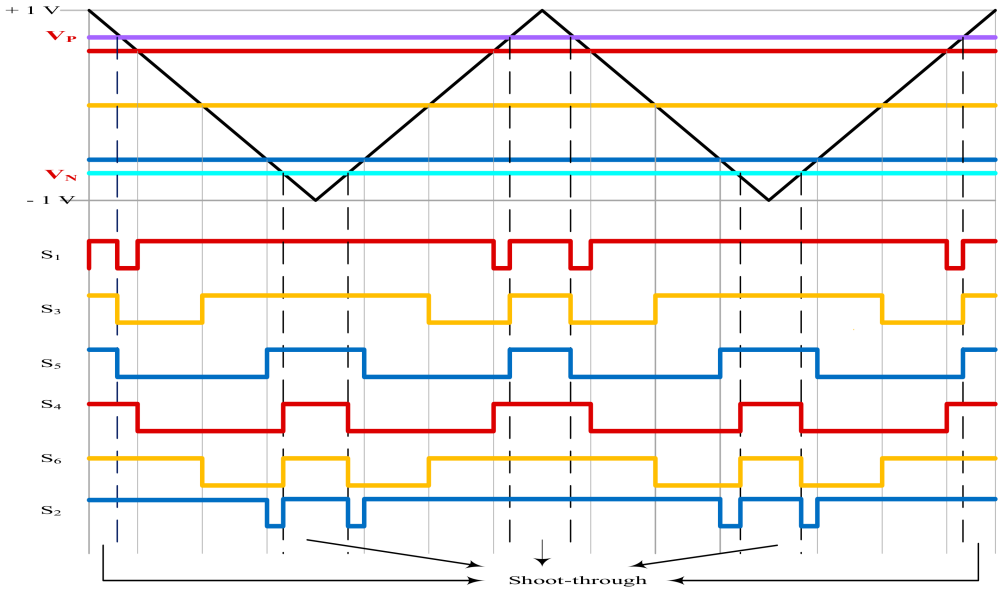


Figure 2. ST pulse generation of the SBPWM switching sequence implemented in the HVB-ZSI.

3.2. Maximum Boost Control PWM (MBCPWM)

MBCPWM is an advanced ST control technique used in ZSIs that maximizes the voltage gain by fully utilizing the available zero states within each switching cycle for ST insertion. MBCPWM achieves this boost without limiting the modulation index, thus ensuring better output-voltage quality and higher DC-link utilization [13]. Figure 3 illustrates the switching diagram of the MBCPWM switching sequence as applied to the HVB-ZSI.

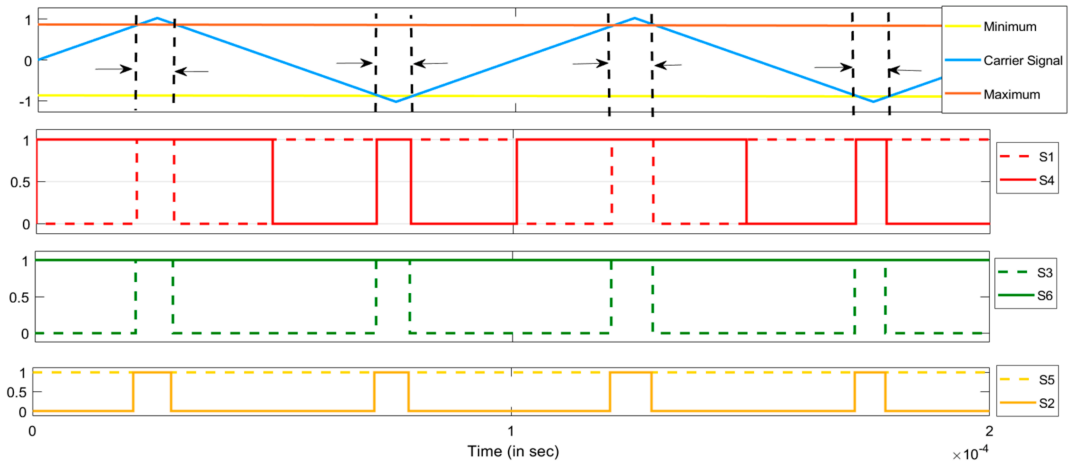


Figure 3. Pulse generation of the MBCPWM switching sequence implemented in the HV−ZSI.

3.3. Third Harmonic Injection-Based Constant Boost Control PWM (THI-CBCPWM)

THI-CBCPWM effectively extends the linear modulation range and allows more time for ST pulse insertion without compromising the amplitude of the output voltage. In this method, d_{st} remains constant throughout the switching cycle, which simplifies control implementation. The key improvement brought by the third-harmonic injection is that it allows the fundamental component of the output to increase to 1.15 due to harmonic injection. This results in better DC bus voltage utilization and reduced THD in the output waveform [14]. The THI-CBCPWM switching sequence utilized in the HVB-ZSI is depicted in Figure 4.

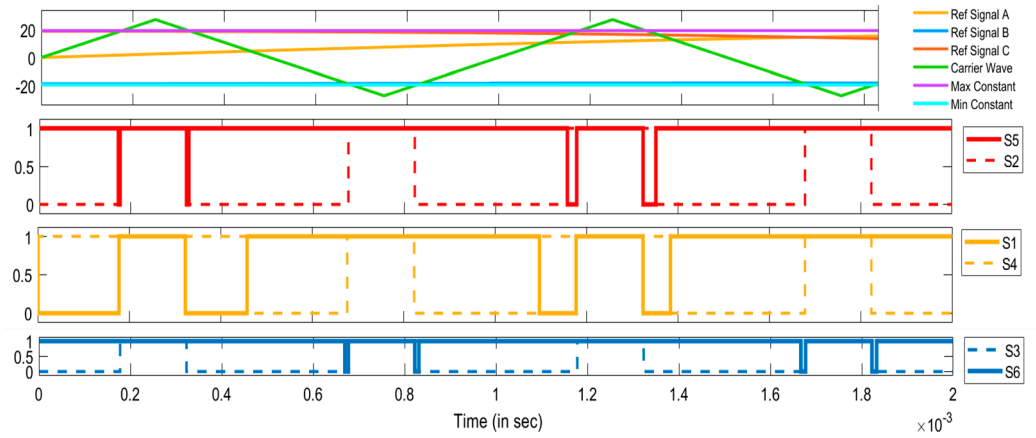


Figure 4. Switching pattern of the THI−CBCPWM switching sequence implemented in the HV−ZSI.

3.4. Space Vector PWM (SVPWM)

This modulation technique enables more precise control of the output waveform and allows for more efficient insertion of ST states. A significant advantage of SVPWM is its ability to maximize the modulation index up to M = 1.1547. Moreover, SVPWM distributes the switching transitions more evenly among the devices, reducing switching losses and thermal stress. This makes it ideal for the HVB-ZSI architecture that seeks not only high voltage gain but also reduced Z-network capacitor stress and limited inrush currents during startup [15,16]. The SVPWM control sequence applied to the HVB-ZSI is illustrated in Figure 5.

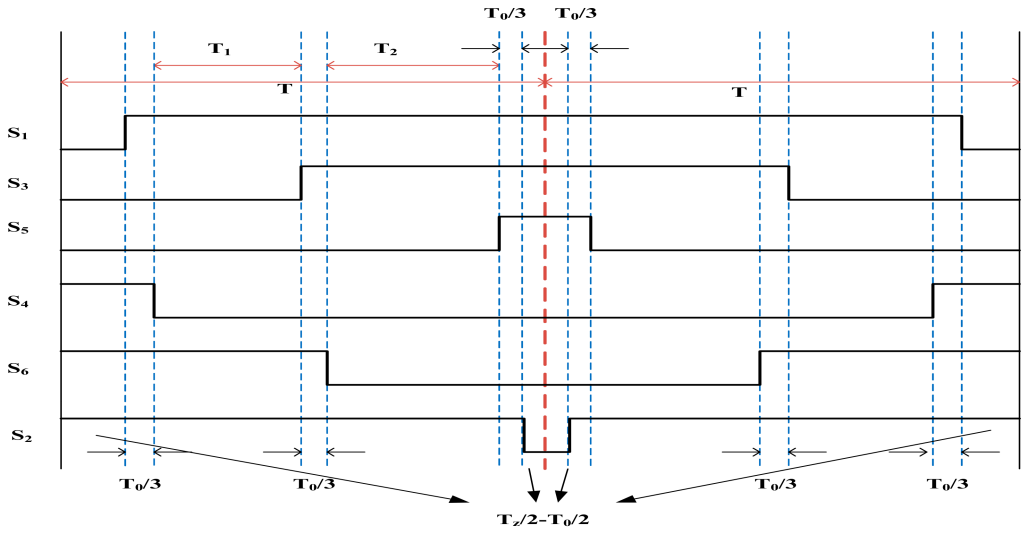


Figure 5. Pulse generation of the SVPWM switching sequence implemented in the HV−ZSI.

4. Comparative Analysis of PWM Techniques for HVB-ZSI Control

The graphical presentation illustrates the analytical relationships between various inverter performance parameters and the modulation index (M). Specifically, Figure 6a shows the variation in duty ratio with modulation index, Figure 6b presents the boost factor versus M, Figure 6c depicts voltage gain versus M, Figure 6d illustrates voltage stress on the topology versus M, and Figure 6e shows capacitor-voltage stress versus M. It is observed that different PWM techniques yield different values of modulation index for the same shoot-through duty cycle. Based on the insights obtained from these graphical analyses, a comparative evaluation of inverter performance parameters has been compiled and presented in Table 1.

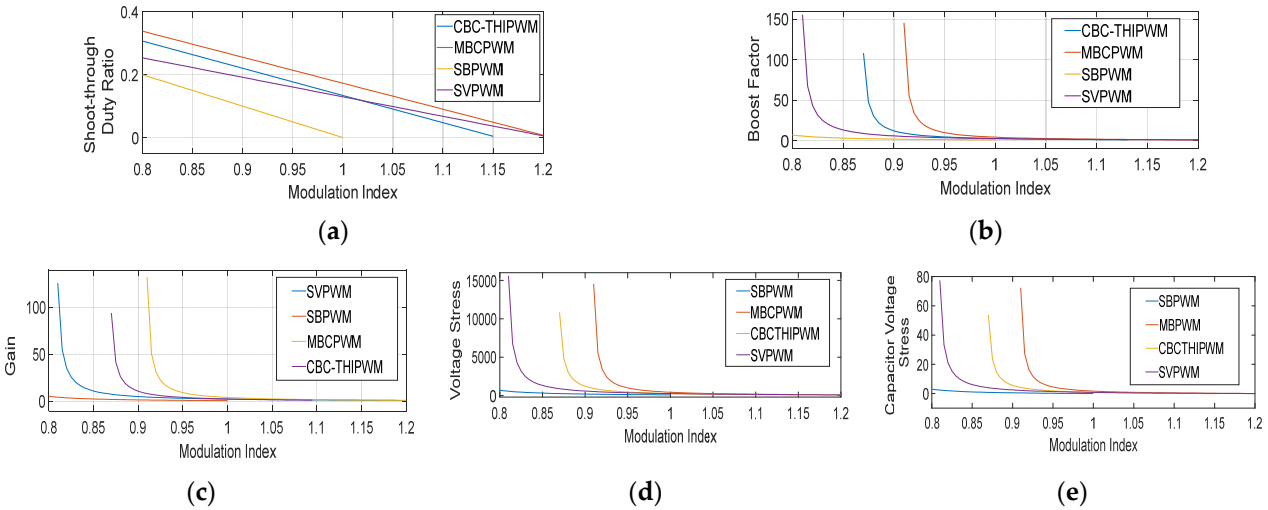


Figure 6. This Graph between (**a**) d_{st} vs. M; (**b**) B vs. M; (**c**) G vs. M; (**d**) Voltage stress on topology vs. M; (**e**) Capacitor-voltage stress vs. M.

Table 1. Comparison table.

Parameters	SBPWM	MBCPWM	THI-CBCPWM	SVPWM
Voltage boost factor, B	$\frac{1+2d_{st}}{1-4d_{st}}$	$\frac{\pi-\sqrt{3}M}{2\sqrt{3}M-\pi}$	$\frac{\sqrt{3}-M}{2M-\sqrt{3}}$	$\frac{10\pi-9\sqrt{3}M}{18\sqrt{3}M-8\pi}$
ST duty ratio, d_{st}	$1-M$	$\frac{2\pi-3\sqrt{3}M}{2\pi}$	$1-\frac{\sqrt{3}M}{2}$	$\frac{3}{4}\times\frac{2\pi-3\sqrt{3}M}{2\pi}$
Capacitor voltage, V_c	$\frac{3(1-M)}{4M-3}$	$\frac{6\pi-9\sqrt{3}M}{12\sqrt{3}M-6\pi}$	$\frac{6-3\sqrt{3}M}{4\sqrt{3}M-6}$	$\frac{18\pi-27\sqrt{3}M}{36\sqrt{3}M-16\pi}$
Gain, G	$M\times B$	$\frac{M\pi-\sqrt{3}M^2}{2\sqrt{3}M-\pi}$	$\frac{\sqrt{3}M-M^2}{2M-\sqrt{3}}$	$\frac{10\pi M-9\sqrt{3}M^2}{18\sqrt{3}M-8\pi}$
Voltage stress on inverter bridge	High	Moderate	Moderate to Low	Moderate
Voltage stress on Z-network capacitor	High	Moderate	Reduced due to TH injection	Moderate
Modulation index range	Up to 1	Up to 1.1	Up to 1.1	Up to ~1.15
Complexity of implementation	Simple	Moderate	Moderate	High

5. Result and Discussion

To evaluate the suitability of different PWM techniques (SBPWM, MBCPWM, THI-CBCPWM, and SVPWM) for this inverter, comparisons should be made based on the quantitative and qualitative criteria. A simulation model of a three-phase HVB-ZSI, configured according to the parameters in Table 2, has been created in MATLAB/Simulink to study its performance across various PWM modulation techniques presented earlier.

Figure 7 demonstrates the enhanced operational performance of the proposed HVB-ZSI [7] compared to conventional ZSI models, as reflected in the improved diode current profile, reduced voltage stress across the active switch, and smoother current transition through the switch, demonstrating the effective current transfer mechanisms and clamping action inherent in the HVB ZSI topology.

Figure 8a–d presents the simulation results for four different PWM techniques: SBPWM, MBCPWM, THI-CBCPWM, and SVPWM. These results include waveforms of the dc-link voltage, one-phase output voltage, inductor current, and capacitor voltage, highlighting the dynamic response of each method. Subsequently, Figure 9a–d provides the FFT analysis of the output line-to-line voltage for the same techniques, allowing for comparison of harmonic distortion levels. Finally, Figure 10 illustrates the ripple current

through the Z-network inductors under each PWM scheme, further emphasizing the impact of the modulation strategy on current quality and overall inverter performance. The THI-CBCPWM technique exhibits the lowest ripple amplitude, indicating more stable inductor current behavior and reduced stress on the passive components. The key observations are included in Table 3.

Table 2. System parameters.

Parameter	Specification
DC supply	100 V
Output frequency	50 Hz
Switching frequency	10 kHz
ST Duty Ratio	0.1925
Z-network capacitor	1200 µF
Z-network inductor	0.5 mH
R_{Load}	15 Ω
L_{Load}	23.13 mH
Power factor	0.9
ST Duty Ratio	0.1925 *

* ST duty ratio taken from reference no. [7].

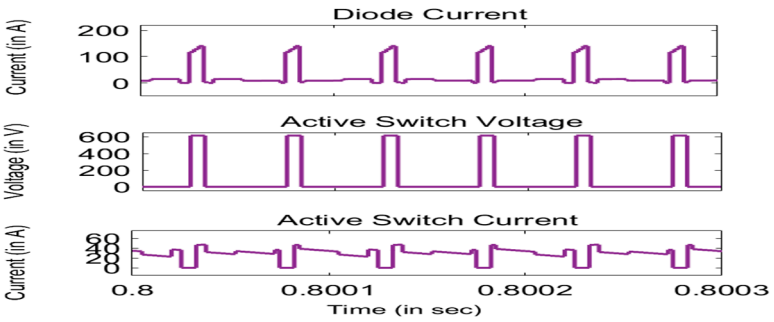


Figure 7. Waveform for diode current, voltage across the active switch (SW_7), and current through the SW_7 switch.

Table 3. HVB-ZSI results with different PWM strategies.

Parameter	SBPWM	MBCPWM	THI-CBCPWM	SVPWM
ST Duty Ratio, d_{st}	0.1925	0.1925	0.1925	0.1925
Modulation Index, M	0.8075	0.977	0.9324	0.8983
DC-link Voltage (V_{in})	613.4 V	603.6	620.3 V	611.4 V
Inductor–Current Ripple (p–p)	2.5 A	37.68 A	2.945 A	6.023 A
Capacitor Voltage (V_c)	210.6 V	251.2 V	213.1 V	151.1 V
Output Voltage THD (%)	71.62%	71.62%	71.62%	66. 25%
Line Current THD (%)	0.94%	0.94%	0.94%	0.89%
V_c, *Peak*	390 V	420 V	385 V	280 V
Inrush Current at stat-up	195 A	250 A	200 A	150 A

https://doi.org/10.3390/engproc2026140007

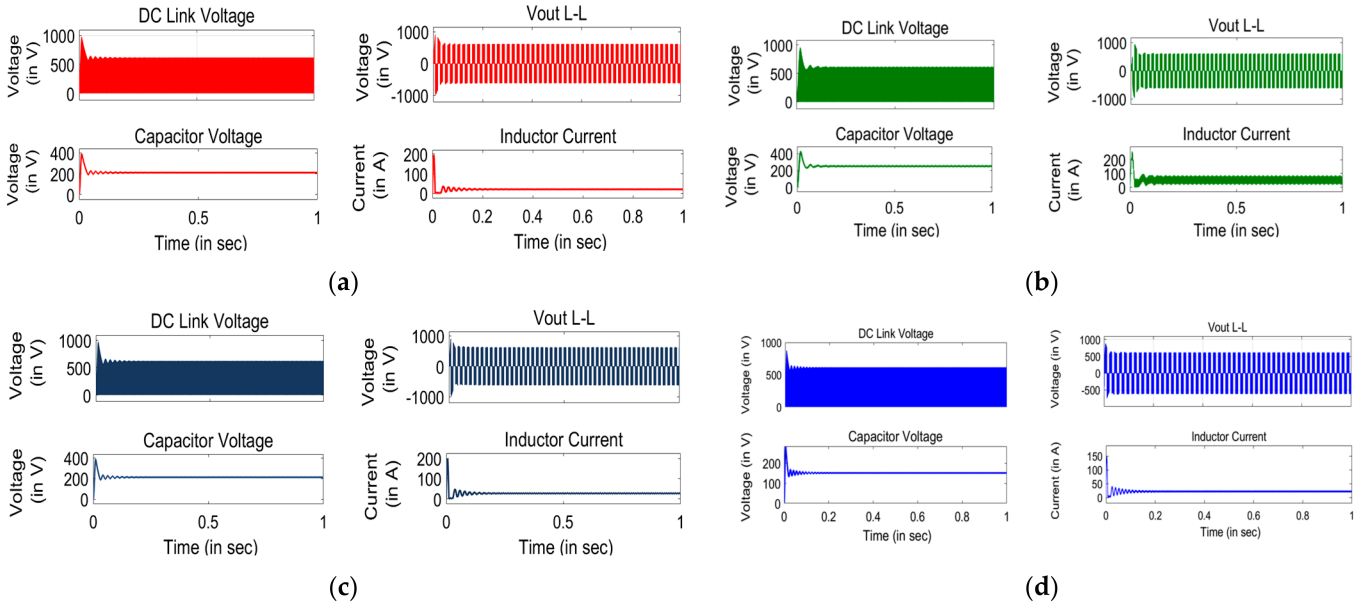


Figure 8. Simulation results in case of (**a**) SBPWM, (**b**) MBCPWM, (**c**) THI−CBCPWM, (**d**) SVPWM.

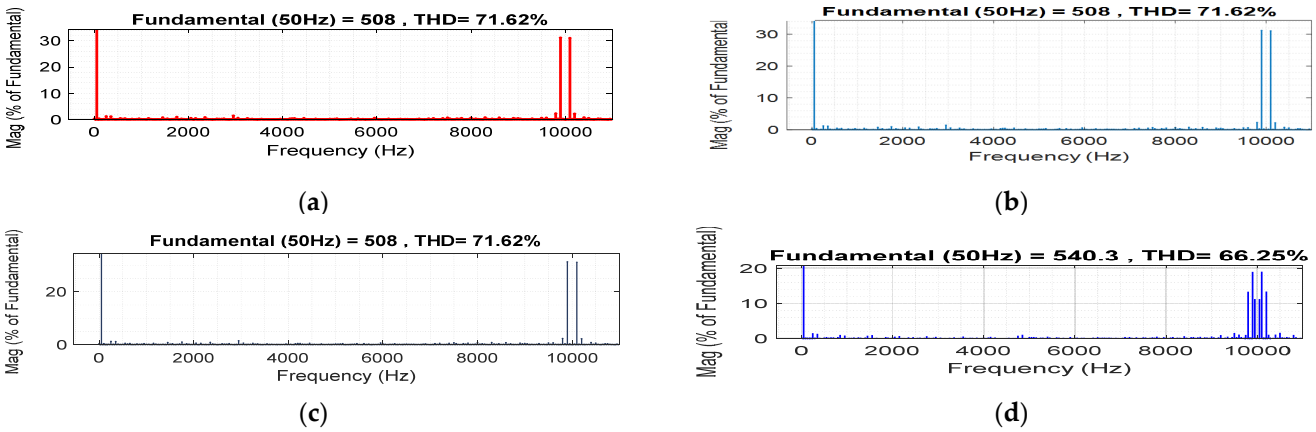


Figure 9. FFT analysis of output line-to-line voltage in case of (**a**) SBPWM, (**b**) MBCPWM, (**c**) THI−CBCPWM, (**d**) SVPWM.

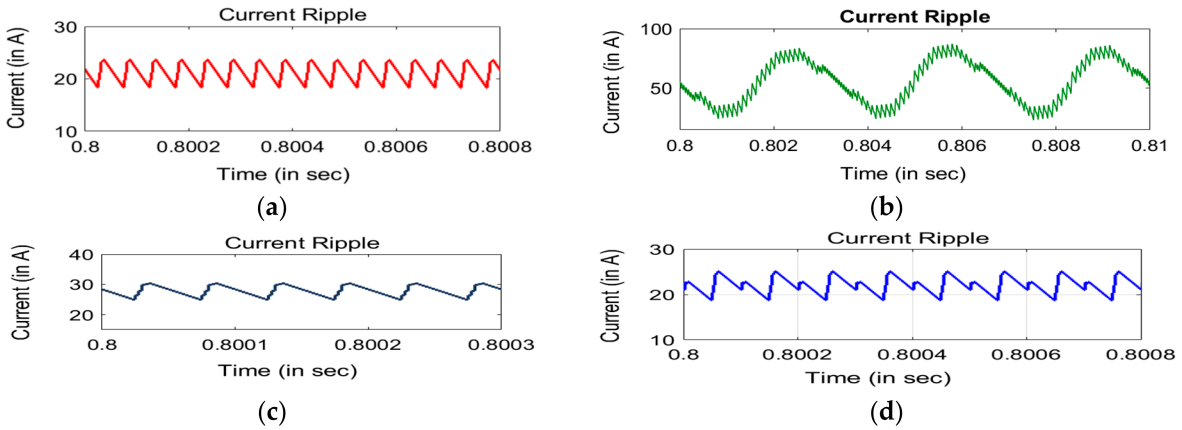


Figure 10. Ripple current through Z-network inductors in case of (**a**) SBPWM, (**b**) MBCPWM, (**c**) THI−CBCPWM, (**d**) SVPWM.

https://doi.org/10.3390/engproc2026140007

6. Conclusions

Simulation results confirm that different PWM strategies significantly impact the HVB-ZSI's performance in terms of voltage gain, shoot-through duty ratio, THD, and device stress. Notably, the THI-CBCPWM technique provides the highest dc-link voltage (620.3 V) and maintains a moderate inductor–current ripple (2.945 A) and a low-line current THD (0.94%), making it suitable for high-voltage applications requiring voltage boosting with acceptable current quality. MBCPWM delivers the highest capacitor voltage (251.2 V) but suffers from excessive inductor current ripple (37.68 A) and high inrush current, which may lead to stress on components. SBPWM and SVPWM show relatively balanced performance; however, SVPWM demonstrates the lowest line-current THD (0.89%) and lowest inrush current (150 A), making it favorable for applications focused on current quality and soft-start behavior. Overall, THI-CBCPWM emerges as the optimal PWM technique for the HVB-ZSI, offering the best compromise between high voltage gain, controlled ripple, and low harmonic distortion, making it highly suitable for renewable energy systems and industrial motor drives where efficient voltage boosting and power quality are critical.

Author Contributions: S.K. was responsible for the conceptualization of the study, development of the model, and execution of simulations. R.K.M. interpreted the results and prepared the initial draft of the manuscript. S.P.D.C. reviewed the manuscript and provided overall supervision and guidance throughout the research work. All authors have read and agreed to the published version of the manuscript.

Funding: This research was funded by the Science and Engineering Research Board (SERB), a statutory body of the Department of Science and Technology, Government of India, under the project titled "Design of Switched-Capacitor Based Boosting Inverter for PV Applications with Fewer Components".

Institutional Review Board Statement: Not applicable.

Informed Consent Statement: Not applicable.

Data Availability Statement: The data supporting the findings of this study are available from the corresponding author upon reasonable request.

Acknowledgments: The authors would like to acknowledge and thank the National Institute of Technology, Patna. Furthermore, we appreciate the support and collaboration with the Independent Institute of Education South Africa (IIEMSA), School of Engineering, Science and Health (SESH), Johannesburg, and S5 Enterprises (Pty) Ltd. for their valuable support and their contributions to the success of this study.

Conflicts of Interest: S.P. Daniel Chowdhury was employed by the S5 Enterprises (Pty) company. The remaining authors declare that the research was conducted in the absence of any commercial or financial relationships that could be construed as a potential conflict of interest.

Abbreviations

The following abbreviations are used in this manuscript:

ST	Shoot-Through
ZSI	Z-source Inverter
HVB-ZSI	High Voltage Boost Z-source Inverter
SBPWM	Simple Boost Pulse Width Modulation
MBCPW	Maximum Boost Control PWM
THI-CBCPWM	Third Harmonic Injection-Based Constant Boost Control PWM
SVPWM	Space Vector PWM

References

1. Gayen, P.K.; Das, S. Wide power control of high-gain and compact quasi-Z-source inverter in remote and sustainable solar water pumping system. *Sustain. Energy Technol. Assess.* **2025**, *74*, 104173. [CrossRef]
2. Sreenu, C.; Mallesham, G.; Sheka, T.C.; Salkuti, S.R. High Gain Quasi Z-Source Converters with Artificial Bee Colony Control for Grid-Integrated Solar-Wind Energy Sources. *Green Energy Intell. Transp.* **2025**, *4*, 100264. [CrossRef]
3. Adnan, M.M.; Sharma, A.; Saravanan, T.; Bhagat, R.K.; Jolad, B.; Naidu, K.K. Advanced Control Strategies for Multilevel Inverters in Renewable Energy Systems: Enhancing Power Quality and Efficiency. *E3S Web Conf.* **2024**, *591*, 01013. [CrossRef]
4. Mousa, H.H.; Mahmoud, K.; Lehtonen, M. Enhancing Renewable Energy Hosting Capacity in Unbalanced Microgrids via Empowering Smart Inverters. *IEEE Access* **2025**, *13*, 17161–17181. [CrossRef]
5. Fang, X.P.; Cui, J.M.; Liu, J.; Cao, M.Y. Detail research on the traditional inverter and Z-source inverter. In *2011 International Conference on Applied Superconductivity and Electromagnetic Devices*; IEEE: Piscataway, NJ, USA, 2011; pp. 318–321. [CrossRef]
6. Zarei, G.; Babaei, E.; Sharifian, M.B.B.; Aghaei, H.; Shokati Asl, E. High voltage gain switched z-source inverter with low current stress. *IET Power Electron.* **2024**, *17*, 38–53. [CrossRef]
7. Gan, S.; Shi, W. An improved Z-Source inverter with high voltage boost ability. *Electr. Eng.* **2022**, *104*, 869–881. [CrossRef]
8. Batkhishig, B.; Da, P.F.; Gonçalves, C.; Pietrini, G.; Nahid-Mobarakeh, B. PWM Techniques for Two-Level Voltage Source Inverters: A Comparative Study. *IEEE Access* **2025**, *13*, 86235–86255. [CrossRef]
9. Jagan, V.; Maheshwaram, B.C.; Usirikapally, M.; Balachandran, P.K.; Reddy, B.N.; Mettu, S.; Dhanamjayulu, C.; Arunkumar, G.; Saranya, K.C.; Khan, B. Analysis of Different PWM Techniques for Enhanced Ultrahigh Gain Z-Network Topology. *Int. Trans. Electr. Energy Syst.* **2024**, *2024*, 6645798. [CrossRef]
10. Noui, S.; Tabbache, B.; Berkouk, E.; Benbouzid, M. A Pulse-Width Modulation Control Approach for the High-Voltage Gain Operation of a Z-Source Neutral-Point Clamped Inverters. *IETE J. Res.* **2023**, *69*, 7374–7393. [CrossRef]
11. Hossameldin, A.A.; Abdelsalam, A.K.; Ibrahim, A.A.; Williams, B.W. Enhanced performance modified discontinuous PWM technique for three-phase Z-source inverter. *Energies* **2020**, *13*, 578. [CrossRef]
12. Thangaprakash, S.; Krishnan, A.; Jothibasu, P.; Kumar, C.S.S. Analysis of Advanced Pulse-Width Modulation Schemes for Z-Source Inverters. *Aust. J. Electr. Electron. Eng.* **2015**, *8*, 155–170. [CrossRef]
13. Khajesalehi, E.; Sheshyekani, J.; Hamzeh, K.; Afjei, M. Maximum constant boost approach for controlling quasi-Z-source-based interlinking converters in hybrid AC–DC microgrids. *IET Gener. Transm. Distrib.* **2016**, *10*, 938–948. [CrossRef]
14. Yadav, S.K.; Mishra, N.; Singh, B. Optimal third harmonic injection based nearest level control of large-scale solar photovoltaic multilevel converter. *Energy Convers. Econ.* **2022**, *3*, 61–71. [CrossRef]
15. El Badsi, I.N.; El Badsi, E. SVM-Based Control of Solar PV-Fed B3 Inverter for Variable Speed Induction Motor Drives. *IEEE Access* **2025**, *13*, 69039–69050. [CrossRef]
16. Mahmoud, Z.B.; Khedher, A. A Comprehensive Review on Space Vector Based-PWM Techniques for Common Mode Voltage Mitigation in photovoltaic Multi-Level inverters. *Energies* **2024**, *17*, 916. [CrossRef]

Disclaimer/Publisher's Note: The statements, opinions and data contained in all publications are solely those of the individual author(s) and contributor(s) and not of MDPI and/or the editor(s). MDPI and/or the editor(s) disclaim responsibility for any injury to people or property resulting from any ideas, methods, instructions or products referred to in the content.